

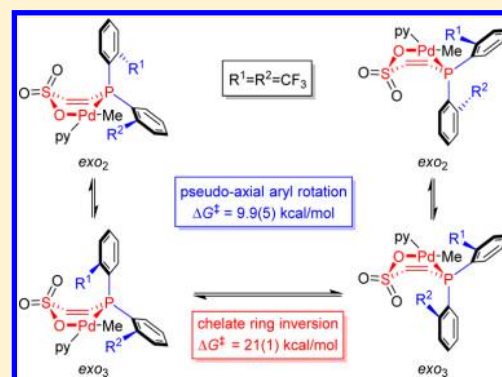
Differentiation between Chelate Ring Inversion and Aryl Rotation in a CF₃-Substituted Phosphine-Sulfonate Palladium Methyl Complex

Ge Feng, Matthew P. Conley, and Richard F. Jordan*

Department of Chemistry, The University of Chicago, 5735 South Ellis Avenue, Chicago, Illinois 60637, United States

Supporting Information

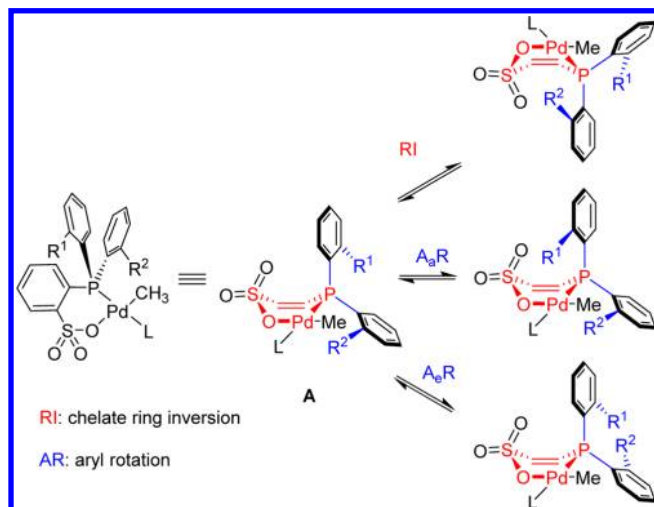
ABSTRACT: The solution conformations and dynamic properties of the CF₃-substituted (*ortho*-phosphinoarenesulfonate)Pd complexes (PO-CF₃)-PdMe(L) ([PO-CF₃]⁻ = 2-[(*o*-CF₃-Ph)₂P]-4-Me-benzenesulfonate, L = 2,6-lutidine (3), pyridine (4)) were studied by NMR spectroscopy, taking particular advantage of ³¹P–¹⁹F through-space couplings and ¹H–¹H and ¹H–¹⁹F nuclear Overhauser effects. In CD₂Cl₂ solution in the temperature range of –80 to 20 °C, 3 adopts an *exo*₂ conformation. One *o*-CF₃-Ph ring is positioned such that the CF₃ group points toward Pd (*exo*) and exhibits through-space ⁴J_{PF} coupling. The other *o*-CF₃-Ph ring is positioned such that the CF₃ group points away from Pd (*endo*) and does not exhibit through-space ⁴J_{PF} coupling, and the *o*-H lies in the deshielding region near an axial site of the Pd square plane and exhibits a low-field chemical shift ($\delta > 9$). Complex 4 exists as a 2:1 mixture of *exo*₂ and *exo*₃ isomers in CD₂Cl₂ solution at –90 °C. In *exo*₂-4, one CF₃ group is *exo* and exhibits through-space ⁴J_{PF} coupling, while the other CF₃ group is *endo* and does not exhibit through-space ⁴J_{PF} coupling. In *exo*₃-4, both CF₃ groups are *exo* and exhibit through-space ⁴J_{PF} couplings. Complex 4 undergoes two dynamic processes: rotation of the axial *o*-CF₃-Ph ring (A_aR), which interconverts *exo*₂-4 and *exo*₃-4 ($\Delta G^\ddagger = 9.9(5)$ kcal/mol), and chelate ring inversion (RI), which permutes the axial and equatorial *o*-CF₃-Ph rings ($\Delta G^\ddagger = 21(1)$ kcal/mol).



INTRODUCTION

Palladium(II) alkyl complexes that contain *ortho*-phosphinoarenesulfonate ligands ([PO]⁻) exhibit unique behavior in olefin polymerization.¹ After the seminal reports by Drent and Pugh in 2002,² (PO)PdR(L) species (L = labile ligand, Scheme 1) have been studied extensively by the groups of Claverie,³

Scheme 1. Possible Dynamic Processes of (PO-CF₃)PdMe(L) Complexes

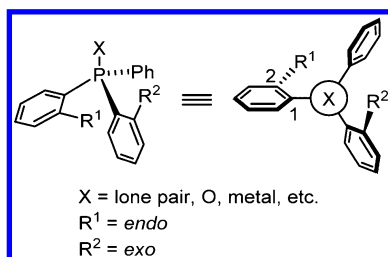


Jordan,⁴ Mecking,⁵ Nozaki,⁶ Rieger,⁷ and others.⁸ These catalysts polymerize ethylene to linear polyethylene and copolymerize ethylene with a variety of polar vinyl monomers to form functionalized linear polymers with functional groups incorporated at both in-chain and chain-end positions. Additionally, (PO)PdR(L) complexes catalyze the nonalternating copolymerization of ethylene and CO^{2b,9} and the alternating copolymerization of CO with vinyl acetate and methyl acrylate.¹⁰

In the solid-state structure of the prototypical (PO)Pd complex (2-[(*o*-OMe-Ph)₂P]-benzenesulfonate)PdMe(py) (Scheme 1, R¹ = R² = OMe),^{9d} the (PO)Pd chelate ring adopts a boat conformation, and the *o*-MeO-Ph rings occupy pseudoaxial and pseudoequatorial positions. Howell and co-workers have developed a simple convention for describing the conformations of Ar₃PX species (X = lone pair, O, or metal) that contain *ortho* substituents on the Ar rings (Scheme 2).¹¹ The Ar ring is designated as *exo* if the *ortho* substituent points toward the X group ($|\theta_{X-P-C1-C2}| < 90^\circ$) and *endo* if it points away from the X group ($|\theta_{X-P-C1-C2}| > 90^\circ$). In (PO)PdMe(L) complexes, the ArSO₃⁻ group is always *exo* because the –SO₃⁻ group coordinates to Pd, but the other two P-Ar rings can be either *exo* or *endo*. In (2-[(*o*-OMe-Ph)₂P]-benzenesulfonate)-PdMe(py) (Scheme 1), the methoxy group on the pseudoaxial

Received: July 3, 2014

Published: August 21, 2014

Scheme 2. *Endo* and *Exo* Conformations in Ar_3PX Species

o-MeO-Ph ring is *endo* (R^1 in A), while that on the pseudoequatorial ring is *exo* (R^2 in A), and therefore the $[\text{PO}]^-$ ligand in this complex adopts an *exo*₂ conformation.

The ^1H NMR spectrum of $(2-\{(o\text{-OMe-Ph})_2\text{P}\}-4\text{-Me-benzenesulfonate})\text{PdMe}(\text{py})$ at -80°C contains two OCH_3 resonances, indicating that exchange of the two methoxy groups is slow on the NMR time scale. However, only one OCH_3 resonance is observed at ambient temperature, indicative of fast methoxy exchange. The barrier for permutation of the methoxy groups is $\Delta G^\ddagger = 10.5$ kcal/mol at -50°C .^{4c} Other $(\text{PO})\text{PdMe}(\text{py})$ complexes that contain *ortho*-substituted *P-Ar* rings exhibit similar dynamic behavior.^{3c,4c}

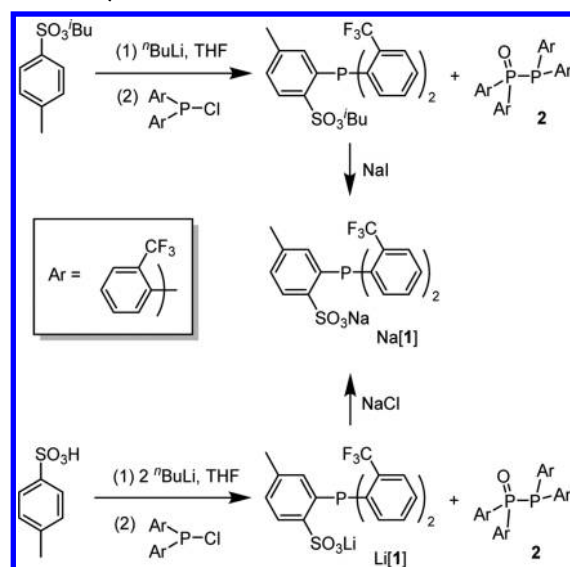
For $(\text{PO})\text{Pd}(\text{R})(\text{L})$ species that contain *ortho*-substituted *P-Ar* groups, several dynamic processes are possible (Scheme 1): chelate ring inversion (RI), which exchanges the pseudoaxial and pseudoequatorial *P-Ar* groups, and rotation of the pseudoaxial and pseudoequatorial *P-Ar* rings around the P-C_{ipso} bonds (A_aR , A_eR), which exchanges the *ortho* substituents between *exo* and *endo* positions. The observation of inequivalent methoxy groups in $(2-\{(o\text{-OMe-Ph})_2\text{P}\}-4\text{-Me-benzenesulfonate})\text{PdMe}(\text{py})$ at -80°C implies that either RI is slow or, if RI is fast, both A_aR and A_eR are slow. The observation of fast methoxy exchange at ambient temperature requires that RI is fast and A_aR and/or A_eR is fast. Note that when RI is fast, A_aR and A_eR cannot be differentiated. Recently Caporaso, Mecking, and co-workers reported an experimental and computational study of the dynamic properties of a series of $[\text{PO}]^-$ salts, $[\text{PO}]\text{H}$ zwitterions, and corresponding “ $(\text{PO})\text{PdMe}$ ” complexes (generated in situ by halide abstraction from the cation-bridged $[(\text{PO})\text{PdMe}(\text{Cl})-\mu\text{-M}]_n$ ($\text{M} = \text{Na}$ or Li) species in CD_3OD or $\text{DMSO}-d_6$ solution).¹² The authors concluded that for “ $[\text{PO}-(o\text{-R-Ph})_2]\text{PdMe}$ ” species in the range of -90 to 130°C chelate ring inversion is always fast, and the inequivalence of *o*-R-Ph rings observed at low temperature is due to slow aryl rotation.¹³

The dynamic properties of $(\text{PO})\text{Pd}(\text{R})(\text{L})$ species may influence their reactivity in several ways. First, it has been proposed that insertion of $(\text{PO})\text{Pd}(\text{R})(\text{ethylene})$ species in ethylene polymerization occurs by initial isomerization of the ground-state *cis*-*P,R* isomer to the *trans*-*P,R* isomer via a five-coordinate ($\kappa^3\text{-P,O,O-PO}$) $\text{Pd}(\text{R})(\text{ethylene})$ intermediate or transition state, followed by migratory insertion.^{4f,6c,14} The rigidity of the $(\text{PO})\text{Pd}$ framework may influence the barrier to this isomerization process. Second, several interesting stereoselective or potentially stereoselective reactions catalyzed by $(\text{PO})\text{Pd}(\text{R})(\text{L})$ complexes have been developed recently, including the asymmetric copolymerization of vinyl acetate and CO catalyzed by Pd complexes bearing a *P*-chiral $[\text{PO}]^-$ ligand^{10c} and the homooligomerization of methyl acrylate catalyzed by “ $(\text{PO})\text{PdMe}$ ” species bearing a series of $[\text{PO}]^-$ ligands.¹³ The dynamic properties of the $(\text{PO})\text{Pd}(\text{R})(\text{L})$ catalysts may influence the stereoselectivity in these reactions.¹³

The objective of the present work was to design a system for which RI and AR could be differentiated. ^{19}F NMR studies have been widely used to probe the solution conformations and dynamic properties of fluorinated organometallic species.¹⁵ Through-space ^{19}F couplings and $^1\text{H}-^{19}\text{F}$ nuclear Overhauser effects (NOEs) can often provide unique information that is otherwise unavailable. In this work we exploited these phenomena to characterize the RI and AR processes in $(\text{PO-CF}_3)\text{PdMe}(\text{py})$ (**4**, $[\text{PO-CF}_3]^- = 2-\{(o\text{-CF}_3\text{-Ph})_2\text{P}\}-4\text{-Me-benzenesulfonate}$).

RESULTS AND DISCUSSION

Synthesis and Solid-State Structure of $\text{Na}[2-\{(o\text{-CF}_3\text{-Ph})_2\text{P}\}-4\text{-Me-benzenesulfonate}]$ ($\text{Na}[\mathbf{1}]$, $\text{Na}[\text{PO-CF}_3]$). $\text{Na}[\mathbf{1}]$ was synthesized by the reaction of $\text{P}(o\text{-CF}_3\text{-Ph})_2\text{Cl}$ with (i) lithiated isobutyl *p*-toluenesulfonate followed by deprotection of the sulfonate ester with NaI or (ii) dilithiated *p*-toluenesulfonic acid followed by cation exchange with NaCl (Scheme 3). The isolated yields for both routes are ca. 65%.

Scheme 3. Synthesis of $\text{Na}[\mathbf{1}]$ 

The major side product for both reactions was $(o\text{-CF}_3\text{-Ph})_2\text{P}(=\text{O})\text{P}(o\text{-CF}_3\text{-Ph})_2$ (**2**). Compound **2** is probably formed by oxidation of $(o\text{-CF}_3\text{-Ph})_2\text{P-P}(o\text{-CF}_3\text{-Ph})_2$ during workup under air; the latter species may form by lithium/halogen exchange of $\text{P}(o\text{-CF}_3\text{-Ph})_2\text{Cl}$ followed by coupling of $\text{LiP}(o\text{-CF}_3\text{-Ph})_2$ and $\text{P}(o\text{-CF}_3\text{-Ph})_2\text{Cl}$ ¹⁶ or by single-electron transfer between $\text{Li}[\text{isobutyl } p\text{-toluenesulfonate}]$ or $\text{Li}_2[p\text{-toluenesulfonic acid}]$ and $\text{P}(o\text{-CF}_3\text{-Ph})_2\text{Cl}$ followed by radical coupling (see Supporting Information).

Slow diffusion of pentane into a wet CH_2Cl_2 solution of $\text{Na}[\mathbf{1}]$ in the presence of 18-crown-6 results in crystallization of $[\text{Na}(18\text{-crown-6})(\text{H}_2\text{O})][\mathbf{1}]$, which was characterized by X-ray diffraction. The $[\text{Na}(18\text{-crown-6})(\text{H}_2\text{O})]^+$ and $[\mathbf{1}]^-$ ions form a dimeric structure that is held together by hydrogen bonds between the H_2O molecules and the ArSO_3^- groups (Figure 1). The hydrogen atoms that are involved in the hydrogen bond network, H10A and H10B, were located, and their positions were refined isotropically. The O10–O1 (2.94 Å) and O10–O2 (2.87 Å) distances are consistent with the presence of hydrogen bonds.¹⁷

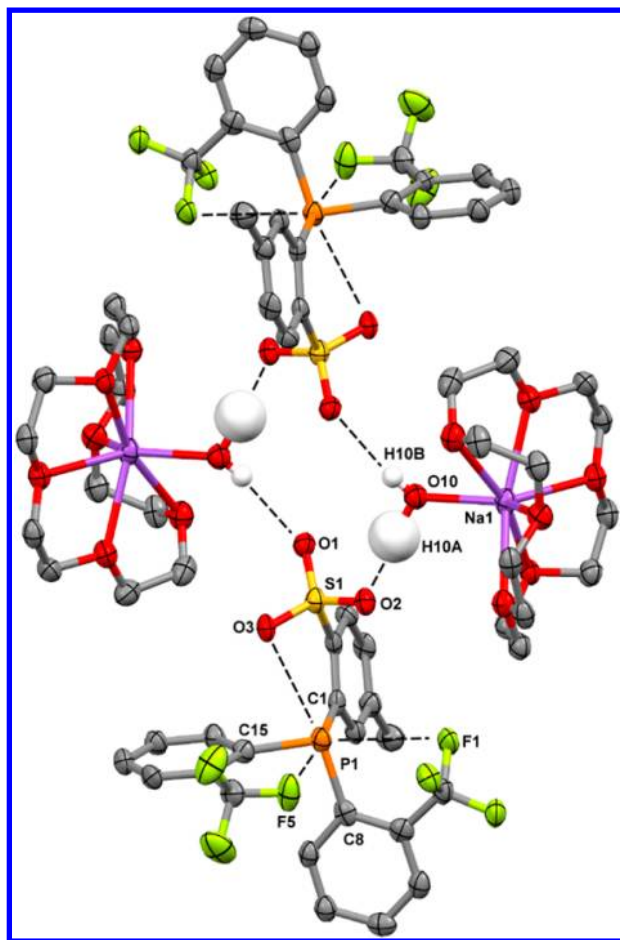


Figure 1. Molecular structure of $[\text{Na}(18\text{-crown-6})(\text{H}_2\text{O})][\mathbf{1}]$. Hydrogen atoms that are not involved in hydrogen bonding are omitted. Selected bond lengths (Å) and angles (deg): P1–C1 1.853(5), P1–C8 1.856(5), P1–C15 1.845(5); C1–P1–C8 100.4(2), C8–P1–C15 98.8(2), C15–P1–C1 102.1(2).

The $[\mathbf{1}]^-$ anion adopts an *exo*₃ propeller conformation in which the aryl rings are rotated ca. 40° off the corresponding (lone pair)–P–C_{ipso} planes in the same direction.¹⁸ The two *o*-CF₃–Ph rings are thus inequivalent. Tris(*ortho*-substituted-aryl)-phosphines normally exhibit *exo*₃ conformations because the *ortho* substituents cause less steric congestion when they point toward the P lone pair (*exo*) rather than toward the other aryl rings (*endo*). For example, P(*o*-CF₃Ph)₃¹⁹ and [HNEt₃][2-((*o*-OMe-Ph)₂P)-benzenesulfonate]²⁰ also have *exo*₃ structures in the solid state.

In $[\text{Na}(18\text{-crown-6})(\text{H}_2\text{O})][\mathbf{1}]$, the P1–F5 (2.774 Å), P1–F1 (2.994 Å), and P1–O3 (2.938 Å) distances are all shorter than the corresponding sums of van der Waals radii (P, F: 3.27 Å; P, O: 3.32 Å),²¹ and the F1–P1–C15 (169°), F5–P1–C1 (176°), and O3–P1–C8 (170°) angles are all close to 180°. Gabbai and co-workers have noted similar features in the zwitterionic species 1-Mes₂FB⁽⁻⁾-2-MePh₂P⁽⁺⁾-benzene and similar compounds and ascribed them to lone-pair(F) → σ*(P–C) interactions.²² Similar lone-pair(F) → σ*(P–C) and lone-pair(O) → σ*(P–C) interactions may be present in $[\text{Na}(18\text{-crown-6})(\text{H}_2\text{O})][\mathbf{1}]$.

Dynamic Properties of $[\mathbf{1}]^-$. The ¹⁹F{¹H} NMR spectrum of Na $[\mathbf{1}]$ in DMSO-*d*₆ at 25 °C consists of two doublets (⁴J_{PF} = 62, 55 Hz), which shows that the two *o*-CF₃–Ph rings are inequivalent on the NMR time scale, consistent with the solid-

state structure. Similar ³¹P–¹⁹F couplings were observed in P(*o*-CF₃–Ph)₃ but not in O=P(*o*-CF₃–Ph)₃,^{19,23} suggesting that these couplings are transmitted through space via lone-pair(F)–lone-pair(P) interactions.^{15c,24} As the temperature is raised, the two doublets broaden and coalesce to one doublet (⁴J_{PF} = 60 Hz, Figure 2). The free energy of activation for this

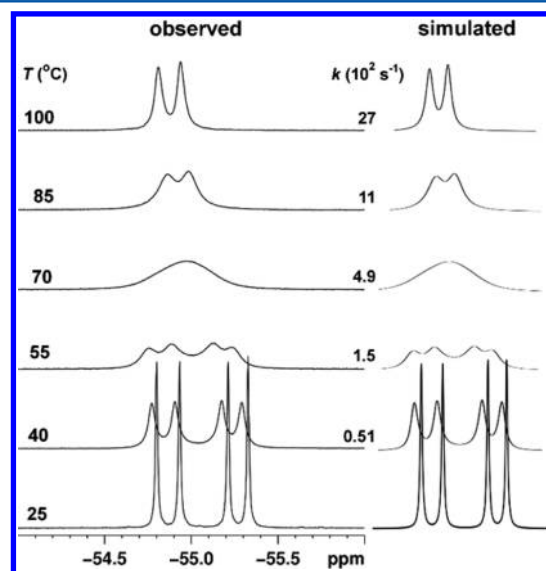


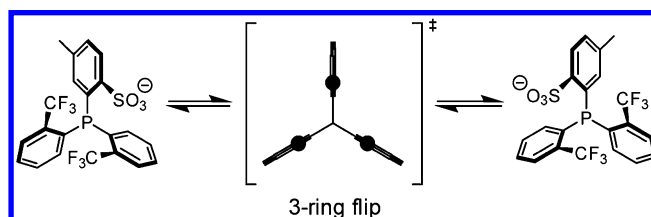
Figure 2. Observed and simulated variable-temperature ¹⁹F{¹H} NMR spectra of Na $[\mathbf{1}]$ in DMSO-*d*₆ solution.

process, $\Delta G^\ddagger = 16.0(4)$ kcal/mol at 55 °C, was determined from a full line shape analysis of these spectra over the temperature range 40–100 °C. A similar value (16.1(5) kcal/mol) was obtained from the coalescence of the H⁶ resonances of the *o*-CF₃–Ph groups in the variable-temperature ¹H NMR spectra (see Supporting Information). A similar barrier (ca. 16 kcal/mol) was reported for Na[2-((*o*-CF₃–Ph)₂P)-benzenesulfonate] in DMSO-*d*₆ solution.¹³

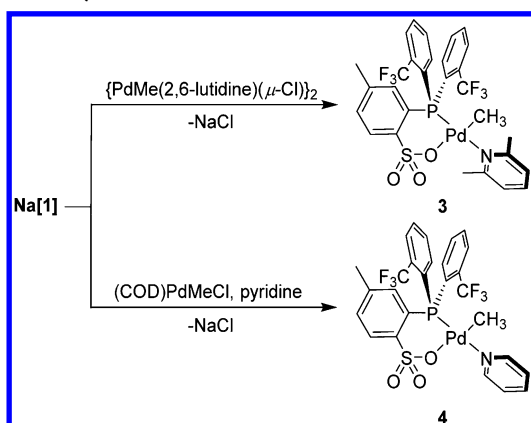
Previous studies by NMR spectroscopy and molecular mechanics computations have shown that tris(*ortho*-substituted-aryl)-phosphines normally adopt *exo*₃ conformations in solution, consistent with their solid-state structures, and that exchange of the *ortho*-substituents occurs via a “three-ring-flip” mechanism, in which all three aryl rings rotate through the corresponding X–P–C_{ipso} planes (i.e., flip) in a concerted manner.^{11,13,19,25} It is likely that the CF₃ groups in $[\mathbf{1}]^-$ also exchange by this mechanism, as illustrated in Scheme 4.

Synthesis and Solid-State Structure of (PO-CF₃)PdMe-(2,6-lutidine) (3). The reaction of Na $[\mathbf{1}]$ with {PdMe(2,6-lutidine)(μ-Cl)}₂ affords (PO-CF₃)PdMe(2,6-lutidine) (3) in 69% isolated yield (Scheme 5). The solid-state structure of 3 (Figure 3) is essentially the same as that of the analogous

Scheme 4. Possible Mechanism for the Exchange of CF₃ Groups in $[\mathbf{1}]^-$



Scheme 5. Synthesis of 3 and 4



(PO)PdMe(2,6-lutidine) complex that contains the 2- $\{(o\text{-CF}_3\text{-Ph})_2\text{P}\}$ -benzenesulfonate ligand.²⁶ In 3, the $[\text{PO-CF}_3]^-$ ligand binds to the square-planar Pd center in a $\kappa^2\text{-P,O}$ mode, and the chelate ring adopts a boat conformation.²⁷ The phosphine exhibits an *exo*₂ conformation in which the ArSO_3^- and the pseudo-equatorial *o*- $\text{CF}_3\text{-Ph}$ (F4, F5, F6) group are *exo* (point toward Pd) and the pseudoaxial *o*- $\text{CF}_3\text{-Ph}$ (F1, F2, F3) group is *endo* (points away from Pd). The *exo*- CF_3 group is positioned below one axial site of the Pd center, and the shortest Pd–F distance (Pd1–F4 3.079(3) Å) is nearly equal to the sum of the van der Waals radii (Pd, F: 3.10 Å).²¹ The other Pd axial site is occupied by the *ortho* hydrogen (H17) of the *endo* *o*- $\text{CF}_3\text{-Ph}$ ring, and the Pd1–H17 distance (2.62 Å) is shorter than the sum of the van der Waals radii (Pd, H: 2.83 Å).²¹ Close M–H contacts involving the *ortho*-hydrogens of arylphosphine ligands are common in square-planar d^8 metal complexes.^{4c,7c,28}

Solution Structure of 3. At -80°C , the ^1H NMR spectrum of 3 in CD_2Cl_2 solution contains one Pd– CH_3 resonance and two equal-intensity lutidine methyl resonances, the $^{31}\text{P}\{^1\text{H}\}$ spectrum comprises a quartet ($^4J_{\text{PF}} = 24$), and the $^{19}\text{F}\{^1\text{H}\}$ spectrum consists of a singlet and a doublet ($^4J_{\text{PF}} = 24$)

of equal intensity. These spectra are essentially unchanged at 25°C . These results show that 3 exists as a single conformer with inequivalent *o*- $\text{CF}_3\text{-Ph}$ units and that rotation around the Pd–N bond is slow on the NMR time scale under these conditions. Only one of the two CF_3 groups is coupled with phosphorus. A detailed analysis, discussed below, shows that it is the *exo*- CF_3 group ($\text{CF}^4\text{F}^5\text{F}^6$) that engages in this $^{31}\text{P}\text{--}^{19}\text{F}$ coupling.

The ^1H NMR spectrum of 3 contains a resonance at δ 9.12 (dd, $J_{\text{PH}} = 18$, $J_{\text{HH}} = 7$) that integrates for 1H. This low-field chemical shift is characteristic for an *ortho* hydrogen of a pseudoaxial P-aryl ring that is positioned in the deshielding region close to an axial site of the Pd square plane.²⁸ Therefore, with reference to the solid-state structure, this resonance is assigned to H17 (Figure 3). The $^1\text{H}\text{--}^1\text{H}$ NOESY spectrum (Figure 4) shows that H17 is close to one of the lutidine- CH_3

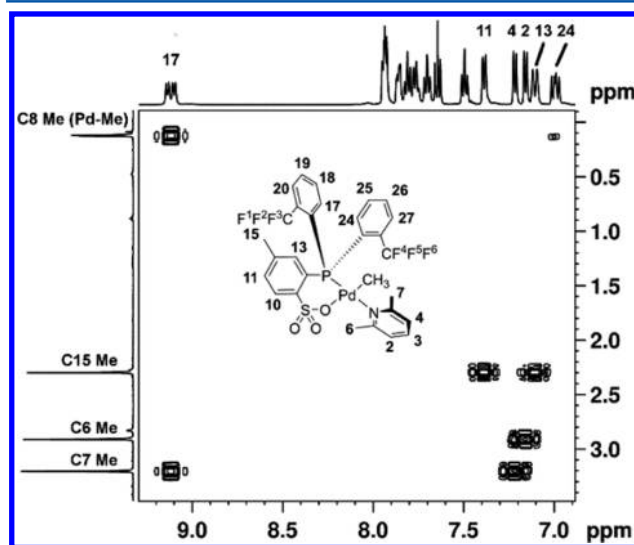


Figure 4. $^1\text{H}\text{--}^1\text{H}$ NOESY spectrum of 3 in CD_2Cl_2 solution.

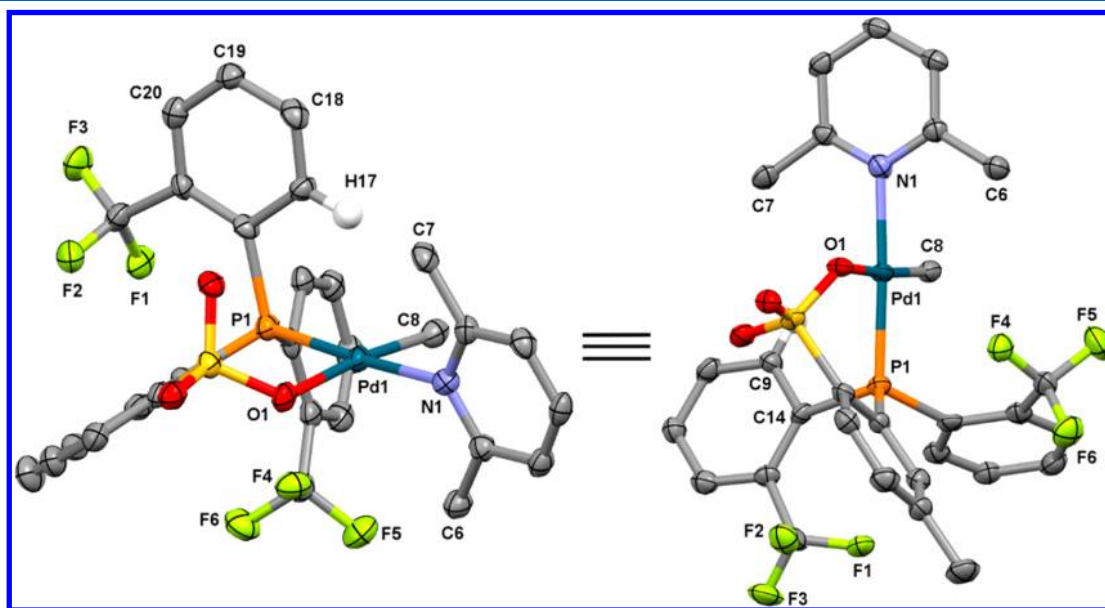


Figure 3. Two views of the molecular structure of 3. Hydrogen atoms except H17 are omitted. Selected bond lengths (Å) and angles (deg): Pd1–P1 2.2343(16), Pd1–O1 2.134(3), Pd1–N1 2.100(4), Pd1–C8 2.001(5), Pd1–F4 3.079(3), Pd1–H17 2.62; P1–Pd1–O1 94.14(10), O1–Pd1–N1 86.98(15), N1–Pd1–C8 89.09(19), C8–Pd1–P1 90.06(15).

groups (C7) and the Pd-CH₃ group (C8), confirming the *exo* conformation of H17. H18–H20 were assigned by the COSY spectrum. The ¹⁹F–¹H HOESY spectrum (Figure 5) shows

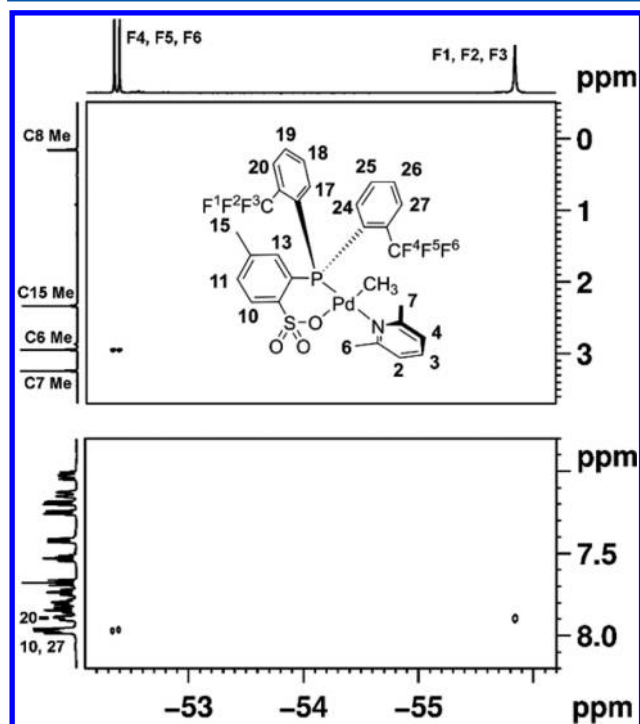
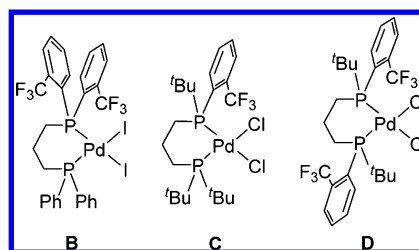


Figure 5. ¹⁹F–¹H HOESY NMR spectrum of **3** in CD₂Cl₂ solution. The ¹H aliphatic region is shown at the top, and the aromatic region is shown at the bottom.

that the ¹⁹F singlet resonance correlates with H20 and therefore corresponds to the *endo*-CF₃ group, i.e., CF¹F²F³. Accordingly, the ¹⁹F doublet is assigned to CF⁴F⁵F⁶. The ¹⁹F–¹H HOESY spectrum also shows that the CF⁴F⁵F⁶ group is close to the other lutidine-CH₃ group (C6) and thus establishes that this CF₃ group is *exo*. Collectively, these NMR results show that the solution structure of **3** is similar to the solid-state structure and features an *exo*₂ conformation of the [PO-CF₃][−] ligand. Furthermore, the observation that ³¹P–¹⁹F coupling is present for the *exo*-CF₃ but not the *endo*-CF₃ group, even though the fluorines on both CF₃ groups are four bonds away from the phosphorus, indicates that this ³¹P–¹⁹F coupling arises by a through-space mechanism. This through-space coupling may arise from overlap of lone-pair(F) and σ(P–Pd) orbitals. Similar ³¹P–³¹P through-space coupling was attributed to lone-pair(P)–σ(P–Pd) interactions.²⁹

An important implication of the NMR analysis of **3** is that for square-planar complexes that contain chelating phosphines with *o*-CF₃-Ph substituents a low-field H⁶ resonance ($\delta > \text{ca. } 9$) and the absence of ⁴J_{PF} coupling are characteristic of an *endo*-CF₃ group, while an H⁶ resonance in the normal range and the presence of ⁴J_{PF} coupling are characteristic of an *exo*-CF₃ group. Data for related compounds (Chart 1) that contain chelating phosphines with *o*-CF₃-Ph substituents are consistent with this trend. For example, in compound **B**,³⁰ one CF₃ group is *exo* and one is *endo* in the solid state. The ¹H NMR spectrum of **B** (CDCl₃) contains a resonance at δ 9.58 that integrates for 1H, and the ¹⁹F{¹H} NMR spectrum comprises a singlet and a doublet. In compound **C**,³¹ the CF₃ group is *endo* in the solid state. The ¹H NMR spectrum of **C** (CD₂Cl₂) contains a

Chart 1. Pd Complexes That Contain Chelating Phosphines with *o*-CF₃-Ph Substituents



resonance at δ 9.30 that integrates for 1H, and the ¹⁹F{¹H} NMR spectrum consists of a singlet. These results indicate that the conformers of the *o*-CF₃-Ph rings are similar in the solid state and solution for **B** and **C**. In compound **D**,³¹ one CF₃ group is *exo* and one is *endo* in the solid state. However, the ¹H NMR spectrum of **D** (CDCl₃) contains a resonance at δ 9.05 that integrates for 2H, and the ¹⁹F{¹H} NMR spectrum consists of one singlet (6F), consistent with *endo* conformation for both *o*-CF₃-Ph rings. In this case, the conformation is different in the solid state and solution.

Dynamic Properties of 3. The ¹H and ¹⁹F{¹H} NMR spectra of **3** in CDCl₂CDCl₂ solution at 100 °C exhibit slight line broadening, which suggests that a slow dynamic process is operative. The ¹⁹F EXSY spectrum at 100 °C (Figure 6)

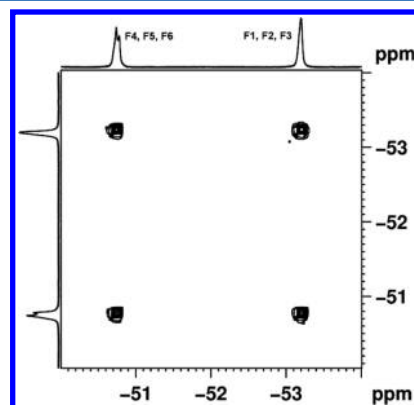


Figure 6. ¹⁹F EXSY spectrum of **3** in CDCl₂CDCl₂ solution at 100 °C.

confirms that the *exo* and *endo* *o*-CF₃-Ph groups undergo exchange. Rate constants for this CF₃ exchange were obtained from quantitative ¹⁹F EXSY experiments over the temperature range of 55 to 100 °C.³² The free energy of activation at 100 °C is $\Delta G^\ddagger = 20.2(4)$ kcal/mol.

Synthesis and Solid-State Structure of (PO-CF₃)PdMe(pyridine) (4). The reaction of Na[**1**] with (COD)PdMeCl in the presence of pyridine affords (PO-CF₃)PdMe(pyridine) (**4**) in 85% isolated yield (Scheme 5). Slow diffusion of pentane into a CH₂Cl₂/benzene solution of **4** results in crystallization of 4·CH₂Cl₂, which was characterized by X-ray diffraction (Figure 7). The molecular structure of **4** is similar to that of **3**. The (PO-CF₃)Pd chelate ring adopts a boat conformation.²⁷ The phosphine adopts an *exo*₂ conformation, with the *exo*-CF₃ group (CF¹F²F³) lying under one Pd axial site (Pd1–F1 3.063(4) Å) and the *ortho* hydrogen of the *endo*-*o*-CF₃-Ph ring lying above the other Pd axial site (Pd1–H22 2.72 Å). However, the dihedral angle between the pyridine plane and the Pd square plane is smaller in **4** ($\theta_{\text{C-Pd-N-C}} 52.8(4)^\circ$) than the corresponding dihedral angle in **3** ($80.3(4)^\circ$).

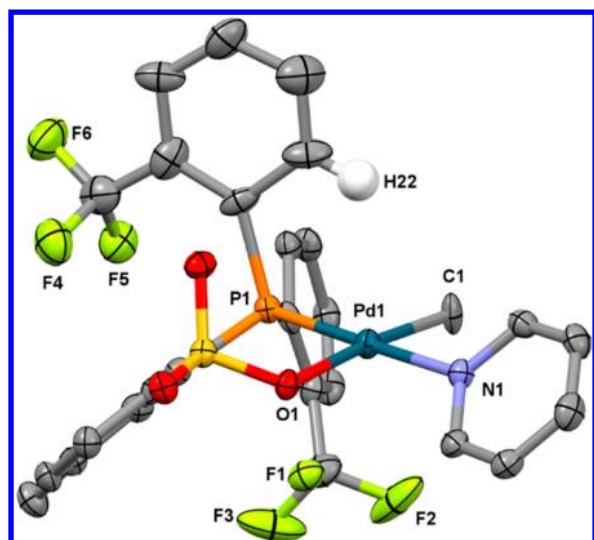


Figure 7. Molecular structure of 4-CH₂Cl₂. Hydrogen atoms except H22 and the CH₂Cl₂ solvent molecule are omitted. Selected bond lengths (Å) and angles (deg): Pd1–P1 2.2174(14), Pd1–O1 2.126(3), Pd1–N1 2.082(4), Pd1–C1 2.059(5), Pd1–F1 3.063(4), Pd1–H22 2.72; P1–Pd1–O1 94.26(9), O1–Pd1–N1 85.61(14), N1–Pd1–C1 90.48(18), C1–Pd1–P1 89.73(14).

Speciation and Structure of 4 in Solution. The ¹H NMR spectrum of 4 in CD₂Cl₂ solution at –90 °C (Figure 8)

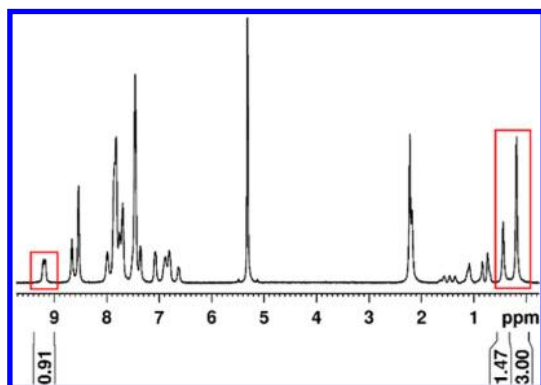


Figure 8. ¹H NMR spectrum of 4 in CD₂Cl₂ solution at –90 °C. Integrations are shown beneath the spectrum.

contains two Pd-CH₃ resonances in a 2:1 intensity ratio, indicating the presence of two isomers. The spectrum contains a doublet at δ 9.19 ($J_{\text{PH}} = 16$ Hz), which is characteristic for the *ortho*-H on an *endo* *o*-CF₃-Ph ring, based on the results for 3 and other d⁸ square-planar complexes. The integrated intensity of this resonance is one-third that of the major Pd-CH₃ resonance, indicating that the major isomer has one *endo* *o*-CF₃-Ph ring. The ³¹P{¹H} NMR spectrum of 4 in CDCl₂F solution at –110 °C (Figure 9) also contains two resonances in a 2.4:1 intensity ratio, confirming the presence of two isomers. The ³¹P{¹H} resonance of the major isomer (δ 45.3) is a quartet ($^4J_{\text{PF}} = 24$ Hz); that is, the phosphorus couples with only one CF₃ group, and so one CF₃ group of this isomer must be *exo*. These results establish that the major isomer of 4 has an *exo*₂ conformation.

The ³¹P{¹H} resonance of the minor isomer of 4 comprises a 10-line multiplet at δ –34.8, corresponding to a quartet of quartets ($^4J_{\text{PF}} = 27, 12$ Hz, simulated by gNMR). The fact that

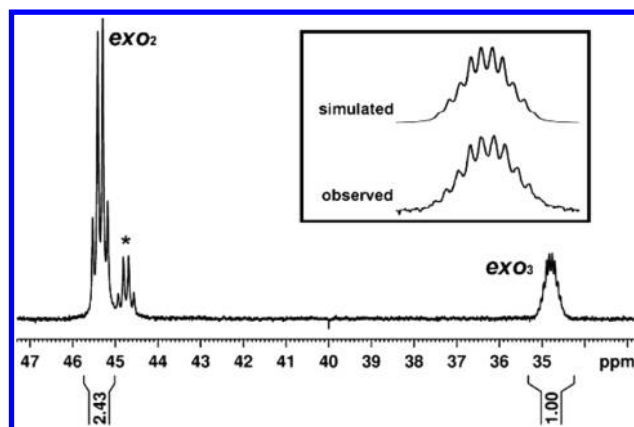


Figure 9. ³¹P{¹H} NMR spectrum of 4 in CDCl₂F solution at –110 °C. Expanded views of the observed and simulated resonance for the *exo*₃ isomer (δ –34.8) are shown in the inset. The asterisk indicates an impurity resonance. Integrations are shown beneath the spectrum.

phosphorus couples to both CF₃ groups indicates that both CF₃ groups are *exo*, and therefore the minor isomer of 4 has an *exo*₃ conformation.³³

Dynamic Properties of 4. As the temperature is raised from –90 °C, the ³¹P{¹H} resonances of *exo*₂-4 and *exo*₃-4 broaden and coalesce, ultimately forming a single broad resonance at δ 40.7 at 20 °C (CD₂Cl₂, Figure 10). These results indicate that the *exo*₂-4 and *exo*₃-4 isomers interconvert on the NMR time scale. The free energy of activation of this process, $\Delta G^\ddagger = 9.9(5)$ kcal/mol at –40 °C, was determined from the coalescence of the two resonances.³⁴ The *exo*₂-4/*exo*₃-4 ratio decreases from 2:1 at –90 °C to ca. 1:1 at 20 °C.

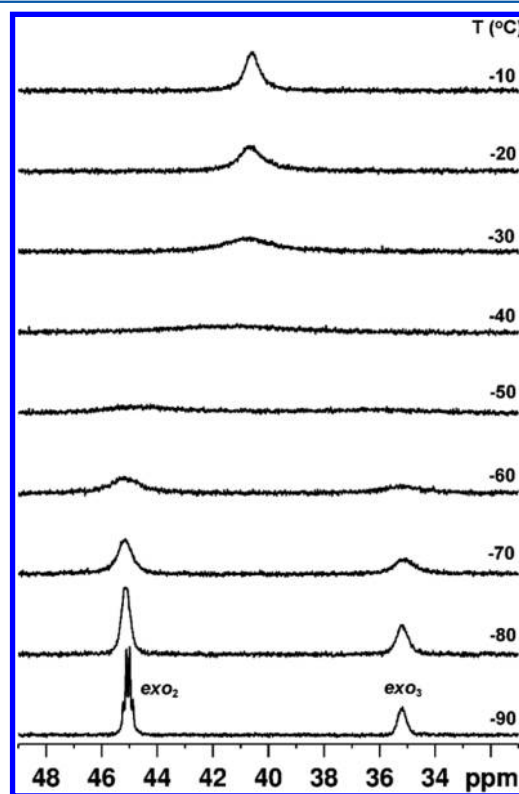


Figure 10. Variable-temperature ³¹P{¹H} NMR spectra of 4 in CD₂Cl₂ solution.

Similarly, the corresponding ^1H NMR resonances for $exo_2\text{-4}$ and $exo_3\text{-4}$ broaden and coalesce as the temperature is raised (Figure 11). The ΔG^\ddagger values determined from the coalescence

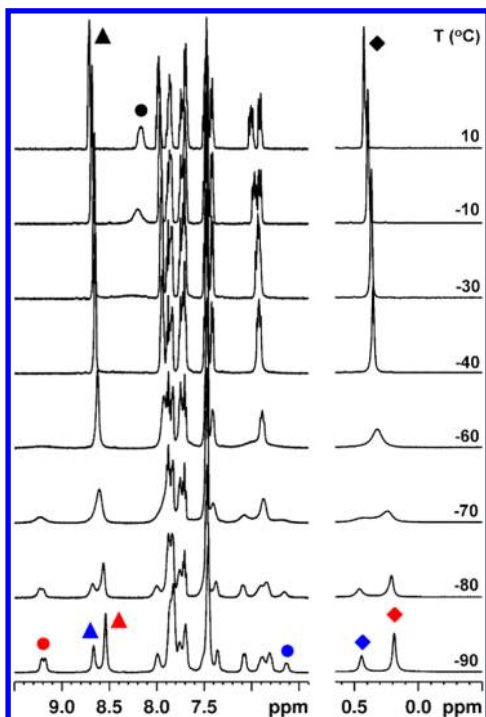


Figure 11. Variable-temperature ^1H NMR spectra of **4** in CD_2Cl_2 solution. The aromatic and Pd- CH_3 regions are shown. Red: $exo_2\text{-4}$, blue: $exo_3\text{-4}$, black: rapidly exchanging $exo_2\text{-4}/exo_3\text{-4}$ mixture. \bullet : $o\text{-CF}_3\text{-Ph-H}^6$, \blacktriangle : $o\text{-py}$, \blacklozenge : Pd- CH_3 .

of the H^6 resonances of the $o\text{-CF}_3\text{-Ph}$ rings (9.7(5) kcal/mol), the *ortho*-H resonances of the pyridine ligand (9.8(5) kcal/mol), and the Pd- CH_3 resonances (9.7(5) kcal/mol) all agree well with the value determined from the $^{31}\text{P}\{^1\text{H}\}$ spectrum.³⁴

The $^{19}\text{F}\{^1\text{H}\}$ NMR spectrum of **4** in CD_2Cl_2 at -90°C (Figure 12) contains four resonances, indicating that the two CF_3 groups within each isomer are inequivalent (trivial for exo_2 , not for exo_3). The resonances at $\delta -51.6$ (d, $^4J_{\text{PF}} = 23$ Hz) and $\delta -56.9$ (s, br) are assigned to the $exo\text{-CF}_3$ and $endo\text{-CF}_3$ groups, respectively, of the major $exo_2\text{-4}$ isomer, based on the relative intensities and similarities of these chemical shifts to those of the corresponding resonances of **3**. The resonances at $\delta -51.9$ (d, $^4J_{\text{PF}} = 27$ Hz) and $\delta -53.2$ (s, br) are assigned to the $exo_3\text{-4}$ isomer.³⁵

As the temperature is raised from -90°C to 20°C , the δ 51.6 resonance of $exo_2\text{-4}$ and the δ 53.2 resonance of $exo_3\text{-4}$ broaden and coalesce, and the δ 56.9 resonance of $exo_2\text{-4}$ and the δ 51.9 resonance of $exo_3\text{-4}$ broaden and coalesce (Figure 12). The ΔG^\ddagger values (9.9(5), 9.8(5) kcal/mol) determined from these two coalescence phenomena agree well with the values derived from the variable-temperature $^{31}\text{P}\{^1\text{H}\}$ and ^1H NMR spectra noted above.³⁴ These results show that the dynamic process that permutes $exo_2\text{-4}$ and $exo_3\text{-4}$ results in exchange of a given $o\text{-CF}_3\text{-Ph}$ group of one isomer with a specific $o\text{-CF}_3\text{-Ph}$ group of the other isomer and are consistent with the sole operation of the A_2R process in this temperature range (Scheme 6).

The $^{19}\text{F}\{^1\text{H}\}$ NMR spectra of the rapidly exchanging $exo_2\text{-4}/exo_3\text{-4}$ mixture in CD_2Cl_2 solution at 20°C (Figure 12) and in

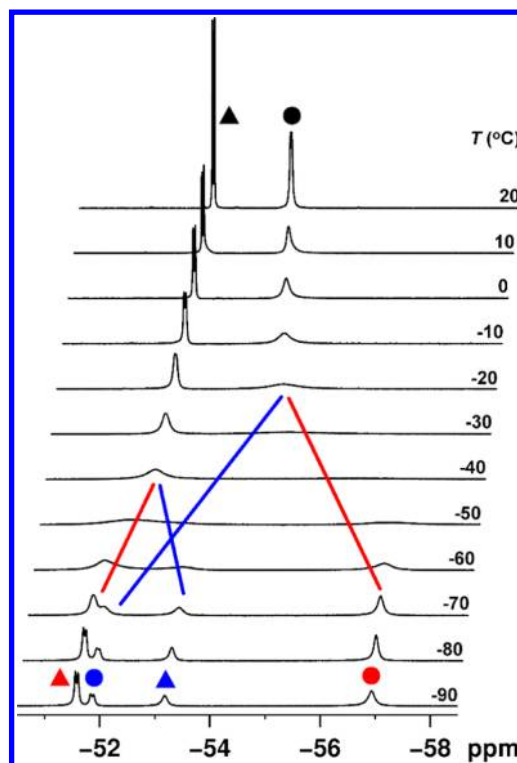


Figure 12. Variable-temperature $^{19}\text{F}\{^1\text{H}\}$ NMR spectra of **4** in CD_2Cl_2 solution. Red: $exo_2\text{-4}$, blue: $exo_3\text{-4}$, black: rapidly exchanging $exo_2\text{-4}/exo_3\text{-4}$ mixture. \bullet : pseudoaxial $o\text{-CF}_3\text{-Ph}$, \blacktriangle : pseudoequatorial $o\text{-CF}_3\text{-Ph}$.

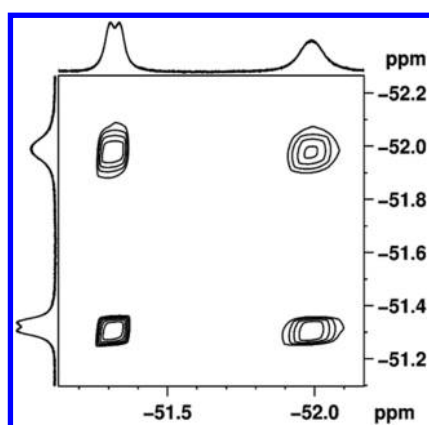
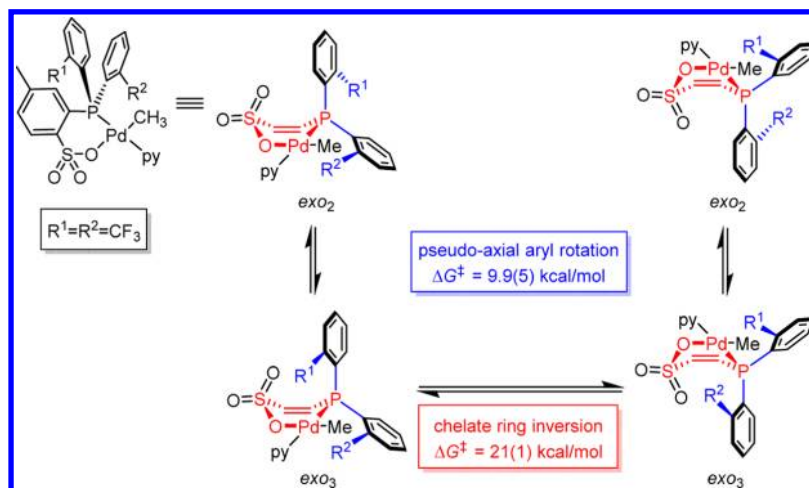
$\text{CDCl}_2\text{CDCl}_2$ solution over the temperature range of 25 to 100°C (Figure S13) contain two resonances of equal intensity. Minor line broadening of these resonances is observed above ca. 70°C , indicative of slow exchange of the CF_3 groups. The CF_3 exchange was confirmed by the ^{19}F EXSY spectrum at 100°C (Figure 13). This CF_3 exchange requires chelate ring inversion (RI). The RI barrier was determined to be $\Delta G^\ddagger(100^\circ\text{C}) = 21(1)$ kcal/mol by quantitative ^{19}F EXSY experiments³² over the temperature range $55\text{--}100^\circ\text{C}$.³⁶

Proposed Mechanism for the Dynamic Processes of **4**.

These dynamic NMR results are most easily explained by the simple exchange mechanism shown in Scheme 6. The low-barrier process ($\Delta G^\ddagger = 9.9(5)$ kcal/mol) that interconverts $exo_2\text{-4}$ and $exo_3\text{-4}$ without exchanging the pseudoaxial and pseudoequatorial $o\text{-CF}_3\text{-Ph}$ rings corresponds to rotation around the P-C bond of the pseudoaxial $o\text{-CF}_3\text{-Ph}$ rings. The higher barrier process ($\Delta G^\ddagger = 21(1)$ kcal/mol), which does exchange the pseudoaxial and pseudoequatorial $o\text{-CF}_3\text{-Ph}$ rings, corresponds to inversion of the $(\text{PO-CF}_3)\text{Pd}$ chelate ring.

Due to the steric congestion around phosphorus, the $exo_2\text{-4}/exo_3\text{-4}$ exchange probably involves some changes in the $(\text{PO-CF}_3)\text{Pd}$ chelate ring conformation and the position of the pseudoequatorial $o\text{-CF}_3\text{-Ph}$ ring, in addition to rotation of the pseudoaxial $o\text{-CF}_3\text{-Ph}$ ring (A_2R). The change in the $^4J_{\text{PF}}$ value for the pseudoequatorial $o\text{-CF}_3\text{-Ph}$ group (23 Hz in $exo_2\text{-4}$, 12 Hz in $exo_3\text{-4}$) likely reflects these additional conformational changes. In fact, these nonzero $^4J_{\text{PF}}$ values do not distinguish whether this CF_3 group is fixed at an *exo* position or undergoes rapid exchange between *exo* and *endo* positions (A_2R in Scheme 1) in $exo_2\text{-4}$ and $exo_3\text{-4}$.

Scheme 6. Proposed Mechanism for the Dynamic Processes of 4

Figure 13. ^{19}F EXSY spectrum of 4 in $\text{CDCl}_2/\text{CDCl}_2$ solution at 100°C .

CONCLUSION

The *exo* and *endo* conformations of the *o*- CF_3 -Ph rings in $(\text{PO}-\text{CF}_3)_2\text{PdMe}(\text{L})$ and related compounds can be identified by NMR. In the *exo* conformation, in which the CF_3 group points toward Pd, through-space J_{PF} coupling is observed. In the *endo* conformation, in which the CF_3 group points away from Pd and the *o*-H is positioned in the deshielding region near an axial site of the Pd square plane, J_{PF} coupling is not observed and the *o*-H ^1H NMR resonance appears at low-field ($\delta > 9$). These trends were exploited to study the solution conformation and dynamic properties of $(\text{PO}-\text{CF}_3)_2\text{PdMe}(\text{py})$ (4). Complex 4 exists as a 2:1 mixture of *exo*₂ and *exo*₃ isomers in CD_2Cl_2 solution at -90°C . In *exo*₂-4, one CF_3 group is *exo* and exhibits through-space $^4J_{\text{PF}}$ coupling, while the other CF_3 group is *endo* and does not exhibit through-space $^4J_{\text{PF}}$ coupling. In *exo*₃-4, both CF_3 groups are *exo* and exhibit through-space $^4J_{\text{PF}}$ couplings. Complex 4 undergoes two dynamic processes: rotation of the pseudoaxial *o*- CF_3 -Ph ring (A_R), which interconverts *exo*₂-4 and *exo*₃-4 ($\Delta G^\ddagger = 9.9(5) \text{ kcal/mol}$), and chelate ring inversion (RI), which permutes the pseudoaxial and pseudoequatorial *o*- CF_3 -Ph rings ($\Delta G^\ddagger = 21(1) \text{ kcal/mol}$).

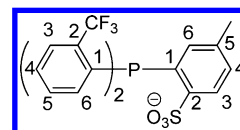
EXPERIMENTAL SECTION

General Procedures. All experiments were performed using glovebox or Schlenk techniques under a N_2 atmosphere unless otherwise noted. N_2 was purified by passage through activated

molecular sieves and Q-5 oxygen scavenger. CD_2Cl_2 and CDCl_3 were distilled from P_2O_5 . CDCl_2F was synthesized by a literature procedure and distilled from P_2O_5 .³⁷ Hexanes, pentane, and toluene were purified by passage through activated alumina and BASF R3-11 oxygen scavenger. Diethyl ether, tetrahydrofuran (THF), and CH_2Cl_2 were purified by passage through activated alumina. $\{\text{PdMe}(\text{2,6-lutidine})(\mu\text{-Cl})\}_2$ was synthesized by a literature procedure.³⁸ *p*-Toluenesulfonic acid was dehydrated from its monohydrate before use.

NMR spectra were recorded in Teflon-valved tubes at ambient probe temperature unless otherwise indicated. ^1H and ^{13}C chemical shifts are reported relative to SiMe_4 and were determined by reference to the residual ^1H and ^{13}C solvent resonances. ^{19}F and ^{31}P NMR spectra were referenced externally to neat CFCl_3 and 85% $\text{H}_3\text{PO}_4/\text{D}_2\text{O}$ ($\delta 0$) respectively. Coupling constants are reported in hertz (Hz). The numbering scheme for NMR assignments is given in Scheme 7.

Scheme 7. Numbering Scheme Used for NMR Assignments



Electrospray mass spectra (ESI-MS) were recorded on freshly prepared samples (ca. 1 mg/mL in CH_2Cl_2 or acetone). In all cases where assignments are given, the observed isotope patterns closely matched calculated isotope patterns. The listed *m/z* value corresponds to the most intense peak in the isotope pattern.

Isobutyl 2-((*o*- CF_3 -Ph)₂P)-4-Me-benzenesulfonate. $^t\text{BuLi}$ (0.39 mL, 2.5 M in hexanes, 0.98 mmol) was added slowly to a solution of ^iBu *p*-toluenesulfonate (0.227 g, 0.995 mmol) in THF (3 mL) at -78°C . The mixture was stirred at -78°C for 3 h. The mixture was added to a solution of (*o*- CF_3 -Ph)₂P-Cl (0.351 g, 0.984 mmol) in diethyl ether (21 mL) at -78°C . The mixture was stirred at -78°C for 3 h and was allowed to warm to 25°C . The mixture was stirred at 25°C for 12 h. The volatiles were removed under vacuum. CH_2Cl_2 was added to afford a white suspension. The mixture was filtered through Celite and concentrated under vacuum to afford a yellow solid, which was purified by flash chromatography (eluant: 15/85 ethyl acetate/hexanes) to yield isobutyl 2-((*o*- CF_3 -Ph)₂P)-4-Me-benzenesulfonate (0.329 g, 0.600 mmol, 61% based on (*o*- CF_3 -Ph)₂P-Cl) as a white solid. ^1H NMR (500 MHz, CDCl_3): δ 8.06 (dd, $J_{\text{HH}} = 8$, $J_{\text{PH}} = 4$, 1H, $\text{H}^3\text{-ArSO}_3$), 7.80–7.76 (m, 2H, $\text{H}^3\text{-ArCF}_3$), 7.52–7.47 (m, 2H, $\text{H}^4\text{-ArCF}_3$), 7.46–7.40 (m, 2H, $\text{H}^5\text{-ArCF}_3$), 7.33 (d, $J_{\text{HH}} = 8$, 1H, $\text{H}^4\text{-ArSO}_3$), 6.94 (s, 2H, $\text{H}^6\text{-ArCF}_3$), 6.66 (s, 1H, $\text{H}^6\text{-ArSO}_3$), 4.07–4.01 (m, 2H, $-\text{OCH}_2-$), 2.26 (s, 3H, ArCH_3), 2.08–1.97 (m, 1H, $-\text{CH}[\text{CH}_3]_2$), 0.96 (d, $J_{\text{HH}} = 7$, 6H, $-\text{CH}[\text{CH}_3]_2$). $^{13}\text{C}\{^1\text{H}\}$ NMR (126 MHz, CDCl_3): δ 144.1 (d, $J_{\text{PC}} = 1$, $\text{C}^5\text{-ArSO}_3$), 138.1 (d, $J_{\text{PC}} =$

27, C²-ArSO₃), 137.0 (s, C⁶-ArSO₃), 136.7 (dd, $J_{PC} = 31$, $J_{FC} = 2$, C¹-ArCF₃), 136.6 (s, C⁶-ArCF₃), 135.8 (s, C⁶-ArCF₃), 135.6 (d, $J_{PC} = 28$, C¹-ArCF₃), 135.5 (d, $J_{PC} = 33$, C¹-ArSO₃), 134.4 (qd, $J_{FC} = 30$, $J_{PC} = 27$, C²-ArCF₃), 133.8 (qd, $J_{FC} = 31$, $J_{PC} = 27$, C²-ArCF₃), 131.9 (s, C⁵-ArCF₃), 131.7 (s, C⁵-ArCF₃), 131.3 (d, $J_{PC} = 4$, C³-ArSO₃), 130.2 (s, C⁴-ArSO₃), 129.5 (s, C⁴-ArCF₃), 129.3 (s, C⁴-ArCF₃), 127.0 (m, C³-ArCF₃), 124.3 (qd, $J_{FC} = 27.5$, $J_{PC} = 2$, ArCF₃), 77.0 (-OCH₂-), 28.3 (-CH[CH₃]₂), 21.7 (ArCH₃), 18.7 (-CH[CH₃]₂). ¹⁹F{¹H} NMR (471 MHz, CDCl₃): δ -57.0 (d, $J_{PF} = 56$), -57.3 (d, $J_{PF} = 54$). ³¹P{¹H} NMR (202 MHz, CDCl₃): δ -13.7 (septet, $J_{PF} = 55$). ESI-MS (MeOH/CH₂Cl₂, 1:1 by volume, positive ion scan, *m/z*): 549.0 (MH⁺). Anal. Calcd for C₂₅H₂₃F₆O₃PS: C, 54.75; H, 4.23. Found: C, 54.72; H, 4.22.

(*o*-CF₃-Ph)₂P(=O)P(*o*-CF₃-Ph)₂ (2). In the flash chromatography described above, after the fractions containing isobutyl 2-((*o*-CF₃-Ph)₂P)-4-Me-benzenesulfonate were collected, the eluant was switched to 30/70 ethyl acetate/hexanes. Fractions containing side products were combined, and volatiles were removed under vacuum to afford a pale yellow solid (0.138 g) as the crude side product. NMR spectra showed that 2 is the major species. Crystals of 2 suitable for X-ray diffraction were obtained by slow diffusion of pentane into a diethyl ether solution of the crude side product. ¹H NMR (500 MHz, acetone-*d*₆): δ 8.68–8.67 (m, 2H), 7.88–7.81 (m, 4H), 7.76–7.73 (m, 4H), 7.70–7.65 (m, 4H), 7.54 (t, $J_{HH} = 7.8$ Hz, 2H). ¹⁹F{¹H} NMR (471 MHz, acetone-*d*₆): δ -55.8 (d, $J_{PF} = 17$, 6F), -56.2 (dd, $J_{PF} = 50$, 5, 6F). ³¹P{¹H} NMR (202 MHz, acetone-*d*₆): δ 40.3 (doublet of septets, $J_{PP} = 243$, $J_{PF} = 5$), -33.0 to -35.7 (m, $J_{PP} = 243$, $J_{PF} = 50$, 17). ESI-MS (MeOH/CH₂Cl₂, 1:1 by volume, positive ion scan, *m/z*): 659.0 (MH⁺).

Na[PO-CF₃] (Na[1]). Route 1. A flask was charged with isobutyl 2-((*o*-CF₃-Ph)₂P)-4-Me-benzenesulfonate (0.38 g, 0.69 mmol), NaI (0.317 g, 2.11 mmol), and CH₃CN (10 mL, purged with N₂ for 20 min before use). The mixture was refluxed for 15 h. The mixture was concentrated under vacuum to afford a white solid, which was washed with H₂O and CHCl₃ to yield Na[1] (0.24 g, 0.47 mmol, 68%) as a white fluffy solid. Crystals of [Na(18-crown-6)(H₂O)][1] suitable for X-ray diffraction were obtained by slow diffusion of pentane into a wet CH₂Cl₂ solution of Na[1] in the presence of 18-crown-6. ¹H NMR (500 MHz, acetone-*d*₆): δ 7.99 (dd, $J_{HH} = 8$, $J_{PH} = 4$, 1H, H³-ArSO₃), 7.81 (s, 1H, H³-ArCF₃(A)), 7.71 (s, 1H, H³-ArCF₃(B)), 7.57–7.55 (m, 1H, H⁴-ArCF₃(A)), 7.51–7.50 (m, 2H, H⁵-ArCF₃(A), H³-ArCF₃(B)), 7.45–7.44 (m, 1H, H⁵-ArCF₃(B)), 7.17 (d, $J_{HH} = 8$, 1H, H⁴-ArSO₃), 7.05 (s, 1H, H⁶-ArCF₃(B)), 6.93 (d, $J_{HH} = 6$, 1H, H⁶-ArCF₃(A)), 6.52 (s, 1H, H⁶-ArSO₃), 2.11 (s, 3H, ArCH₃). ¹³C{¹H} NMR (126 MHz, acetone-*d*₆): δ 148.8 (d, $J_{PC} = 26$, C²-ArSO₃), 139.8 (d, $J_{PC} = 1$, C⁵-ArSO₃), 139.5 (s, C¹-ArCF₃), 139.0 (d, $J_{PC} = 30$, C¹-ArCF₃), 137.7 (s, C⁶-ArCF₃(A)), 136.7 (s, C⁶-ArCF₃(B)), 135.9 (s, C⁶-ArSO₃), 134.8 (dq, $J_{PC} = 31$, $J_{FC} = 28$, C²-ArCF₃), 133.4 (d, $J_{PC} = 27$, C¹-ArSO₃), 133.2–132.7 (m, C²-ArCF₃), 132.6 (s, C⁵-ArCF₃), 132.4 (s, C⁵-ArCF₃), 130.1 (s, C⁴-ArSO₃), 129.8 (s, C⁴-ArCF₃(A)), 129.6 (d, $J_{PC} = 4$, C³-ArSO₃), 129.3 (s, C⁴-ArCF₃(B)), 127.2 (dq, $J_{PC} = 6$, $J_{FC} = 5$, C³-ArCF₃), 125.6 (q, $J_{FC} = 27.5$, ArCF₃), 125.4 (q, $J_{FC} = 27.5$, ArCF₃), 21.18 (s, ArCH₃). ¹⁹F{¹H} NMR (471 MHz, acetone-*d*₆): δ -55.9 (d, $J_{PF} = 61$), -56.4 (d, $J_{PF} = 54$). ³¹P{¹H} NMR (202 MHz, acetone-*d*₆): δ -14.1 (septet, $J_{PF} = 57$). ESI-MS (acetonitrile, positive ion scan, *m/z*): 493.0 (M - Na⁺ + 2H⁺). Multiple elemental analyses on spectroscopically pure samples of this compound did not yield satisfactory results.

Na[1]. Route 2. ⁿBuLi (7.0 mL, 2.9 M in hexanes, 20 mmol) was added slowly to a solution of *p*-toluenesulfonic acid (1.64 g, 9.52 mmol) in THF (25 mL) at -78 °C. The mixture was stirred at -78 °C for 4.5 h. The mixture was added to a solution of (*o*-CF₃-Ph)₂P(=O)Cl (3.39 g, 9.51 mmol) in diethyl ether (25 mL) at -78 °C. The mixture was stirred at -78 °C for 3 h and was allowed to warm to 25 °C. The mixture was stirred at 25 °C for 12 h. The volatiles were removed under vacuum. CH₂Cl₂ (20 mL) and H₂O (20 mL) were added. The aqueous phase was acidified to pH = 2 by adding aqueous HCl solution and then separated. Aqueous NaCl solution was added to the aqueous phase to afford white precipitates. The mixture was filtered to yield Na[1] (3.18 g, 6.18 mmol, 65%) as a white fluffy solid.

(*PO*-CF₃)Pd(Me)(2,6-lutidine) (3). A flask was charged with Na[1] (0.240 g, 0.467 mmol), {PdMe(2,6-lutidine)(μ-Cl)}₂ (0.121 g, 0.229 mmol), and CH₂Cl₂ (7 mL). The mixture was stirred at 25 °C for 6 h. The mixture was filtered. CH₂Cl₂ (8 mL) was used to wash the precipitate and combined with the filtrate. The filtrate was concentrated under vacuum to afford a pale yellow solid, which was recrystallized from CH₂Cl₂/pentane to yield 3 (0.228 g, 0.317 mmol, 69% based on {PdMe(2,6-lutidine)(μ-Cl)}₂) as a pale yellow solid. Crystals of 3 suitable for X-ray diffraction were obtained by slow diffusion of pentane into a CH₂Cl₂ solution of 3. ¹H NMR (500 MHz, CD₂Cl₂): δ 9.12 (dd, $J_{PH} = 18$, $J_{HH} = 7$, 1H, H⁶-ArCF₃(A)), 7.95–7.91 (m, 2H, H³-ArCF₃(B), H³-ArSO₃), 7.87–7.85 (m, 1H, H³-ArCF₃(A)), 7.81 (t, $J_{HH} = 7$, 1H, H⁵-ArCF₃(A)), 7.76 (t, $J_{HH} = 7$, 1H, H⁴-ArCF₃(A)), 7.70 (t, $J_{HH} = 7$, 1H, H⁴-ArCF₃(B)), 7.64 (t, $J_{HH} = 8$, 1H, H⁴-lutidine), 7.49 (t, $J_{HH} = 8$, 1H, H⁵-ArCF₃(B)), 7.38 (d, $J_{HH} = 8$, 1H, H⁴-ArSO₃), 7.22 (d, $J_{HH} = 8$, 1H, H³(A)-lutidine), 7.16 (d, $J_{HH} = 8$, 1H, H³(B)-lutidine), 7.10 (d, $J_{PH} = 12$, 1H, H⁶-ArSO₃), 6.99 (dd, $J_{PH} = 12$, $J_{HH} = 8$, 1H, H⁶-ArCF₃(B)), 3.20 (s, 3H, CH₃(A)-lutidine), 2.91 (s, 3H, CH₃(B)-lutidine), 2.30 (s, 3H, ArCH₃), 0.11 (d, $J_{PH} = 3$, 3H, PdCH₃). ¹³C{¹H} NMR (126 MHz, CD₂Cl₂): δ 159.32 (d, $J_{PC} = 1$, C²-lutidine), 159.25 (d, $J_{PC} = 1$, C²-lutidine), 146.3 (d, $J_{PC} = 16$, C²-ArSO₃), 143.3 (d, $J_{PC} = 28$, C⁶-ArCF₃(A)), 139.7 (d, $J_{PC} = 7$, C⁵-ArSO₃), 139.0 (s, C⁴-lutidine), 136.5 (d, $J_{PC} = 5$, C⁶-ArCF₃(B)), 135.8 (s, C⁶-ArSO₃), 133.7–133.2 (m, C²-ArCF₃), 132.9–132.6 (m, C²-ArCF₃), 132.3 (d, $J_{PC} = 3$, C⁴-ArSO₃), 132.2 (d, $J_{PC} = 2$, C⁴-ArCF₃(A)), 132.1 (d, $J_{PC} = 17$, C⁵-ArCF₃(A)), 131.9 (d, $J_{PC} = 7$, C⁵-ArCF₃(B)), 131.8 (d, $J_{PC} = 2$, C⁴-ArCF₃(B)), 130.0–129.8 (m, C³-ArCF₃(B)), 129.4 (d, $J_{PC} = 44$, C¹-ArCF₃(A)), 128.9–128.8 (m, C³-ArCF₃(A)), 128.4 (d, $J_{PC} = 9$, C³-ArSO₃), 126.8 (d, $J_{PC} = 40$, C¹-ArCF₃(B)), 126.5 (d, $J_{PC} = 45$, C¹-ArSO₃), 124.9 (q, $J_{FC} = 27.6$, ArCF₃), 123.7 (q, $J_{FC} = 27.4$, ArCF₃), 123.2 (d, $J_{PC} = 3$, C³(A)-lutidine), 123.1 (d, $J_{PC} = 3$, C³(B)-lutidine), 27.0 (s, CH₃(A)-lutidine), 26.3 (s, CH₃(B)-lutidine), 21.2 (s, ArCH₃), -4.4 (s, PdCH₃). ¹⁹F{¹H} NMR (471 MHz, CD₂Cl₂): δ -52.3 (d, $J_{PF} = 22$, ArCF₃(B)), -55.7 (s, ArCF₃(A)). ³¹P{¹H} NMR (202 MHz, CD₂Cl₂): δ 41.6 (q, $J_{PF} = 21$). ESI-MS (MeOH/H₂O, 1:1 by volume, positive ion scan, *m/z*): 720.0 (MH⁺). Anal. Calcd for C₂₉H₂₆F₆NO₃PPdS: C, 48.38; H, 3.64; N, 1.95. Found: C, 48.10; H, 3.61; N, 1.62.

(*PO*-CF₃)Pd(Me)(pyridine) (4). A flask was charged with Na[1] (0.132 g, 0.257 mmol), (COD)PdMeCl (0.071 g, 0.27 mmol), pyridine (22 μL, 0.27 mmol), and CH₂Cl₂ (23 mL). The mixture was stirred at 25 °C for 2 h. The mixture was filtered and concentrated under vacuum to afford a pale yellow solid, which was recrystallized from CH₂Cl₂/pentane to yield 4 (0.152 g, 0.220 mmol, 85% based on Na[1]) as a pale yellow solid. Crystals of 4·CH₂Cl₂ suitable for X-ray diffraction were obtained by slow diffusion of pentane into a CH₂Cl₂/benzene solution of 4. ¹H NMR (500 MHz, CD₂Cl₂): δ 8.73 (d, $J_{HH} = 5$, 2H, H²-pyridine), 8.16 (dd, $J_{PH} = 15$, $J_{HH} = 7$, 1H, H⁶-ArCF₃(A)), 8.02–7.97 (m, 2H, H³-ArCF₃(B), H³-ArSO₃), 7.89–7.86 (m, 2H, H³-ArCF₃(A), H⁴-pyridine), 7.77–7.67 (m, 3H, H⁴-ArCF₃(A), H⁴-ArCF₃(B), H⁵-ArCF₃(A)), 7.52–7.45 (m, 3H, H⁵-ArCF₃(A), H³-pyridine), 7.43 (d, $J_{HH} = 8$, 1H, H⁴-ArSO₃), 7.03 (dd, $J_{PH} = 12$, $J_{HH} = 8$, 1H, H⁶-ArCF₃(B)), 6.92 (d, $J_{PH} = 12$, 1H, H⁶-ArSO₃), 2.27 (s, 3H, ArCH₃), 0.45 (s, 3H, PdCH₃). ¹³C{¹H} NMR (126 MHz, CD₂Cl₂): δ 150.8 (s, C²-pyridine), 146.9 (d, $J_{PC} = 15$, C²-ArSO₃), 140.5 (d, $J_{PC} = 19$, C⁶-ArCF₃(A)), 140.2 (d, $J_{PC} = 7$, C⁵-ArSO₃), 138.9 (s, C⁴-pyridine), 136.4 (d, $J_{PC} = 4$, C⁶-ArCF₃(B)), 135.2 (s, C⁶-ArSO₃), 134.0 (qd, $J_{FC} = 31$, $J_{PC} = 10$, C²-ArCF₃), 133.2 (qd, $J_{FC} = 32$, $J_{PC} = 3$, C²-ArCF₃), 132.6 (d, $J_{PC} = 2$, C⁴-ArSO₃), 132.5–132.3 (m, C⁵-ArCF₃), 132.2 (d, $J_{PC} = 2$, C⁴-ArCF₃), 131.9 (d, $J_{PC} = 2$, C⁴-ArCF₃), 129.4 (dq, $J_{PC} = 7$, $J_{FC} = 5$, C³-ArCF₃), 129.3–129.2 (m, C³-ArCF₃), 129.2 (d, $J_{PC} = 9$, C³-ArSO₃), 128.0 (d, $J_{PC} = 43$, C¹-ArCF₃/C¹-ArSO₃), 127.7 (d, $J_{PC} = 43$, C¹-ArCF₃/C¹-ArSO₃), 126.4 (d, $J_{PC} = 47$, C¹-ArCF₃), 125.7 (s, C³-pyridine), 124.7 (qd, $J_{FC} = 27.6$, $J_{PC} = 1$, ArCF₃), 124.2 (qd, $J_{FC} = 27.6$, $J_{PC} = 1$, ArCF₃), 21.2 (s, ArCH₃), 1.7 (s, PdCH₃). ¹⁹F{¹H} NMR (471 MHz, CD₂Cl₂): δ -52.7 (d, $J_{PF} = 18$, ArCF₃(B)), -54.1 (d, $J_{PF} = 8$, ArCF₃(A)). ³¹P{¹H} NMR (202 MHz, CD₂Cl₂): δ 40.7 (br). ESI-MS (MeOH/CH₂Cl₂, 1:1 by volume, positive ion scan, *m/z*): 691.9 (MH⁺). Multiple elemental analyses on

spectroscopically pure samples of this compound did not yield satisfactory results.

X-ray Crystallography. Full details are provided in the Supporting Information. Data were collected on a Bruker Smart Apex diffractometer using Mo K α radiation (0.710 73 Å). Direct methods were used to locate many atoms from the E-map. Repeated difference Fourier maps enabled location of all expected non-hydrogen atoms. Following anisotropic refinement of all non-H atoms, ideal H atom positions were calculated. Final refinement was anisotropic for all non-H atoms and isotropic-riding for H atoms. ORTEP diagrams are drawn with 50% probability ellipsoids.

■ ASSOCIATED CONTENT

■ Supporting Information

Crystal structure report for compounds [Na(18-crown-6)-(H₂O)][1], **2**, **3**, and **4**·CH₂Cl₂; synthesis of compounds; generation and structure of **2**; additional NMR spectra and analysis of Na[**1**] and **4**; details of ¹⁹F EXSY analysis of **3** and **4**; NMR spectra of compounds and crystallographic data in CIF format. This material is available free of charge via the Internet at <http://pubs.acs.org>.

■ AUTHOR INFORMATION

Corresponding Author

*E-mail: rfjordan@uchicago.edu.

Notes

The authors declare no competing financial interest.

■ ACKNOWLEDGMENTS

We thank Antoni Jurkiewicz, Ian Steele, and Jin Qin for assistance with NMR spectroscopy, X-ray crystallography, and mass spectrometry, respectively. This work was supported by the National Science Foundation (grants CHE-0911180 and CHE-1048528).

■ REFERENCES

- (1) (a) Berkefeld, A.; Mecking, S. *Angew. Chem., Int. Ed.* **2008**, *47*, 2538. (b) Nakamura, A.; Ito, S.; Nozaki, K. *Chem. Rev.* **2009**, *109*, 5215. (c) Nakamura, A.; Anselment, T. M. J.; Claverie, J.; Goodall, B.; Jordan, R. F.; Mecking, S.; Rieger, B.; Sen, A.; van Leeuwen, P. W. N. M.; Nozaki, K. *Acc. Chem. Res.* **2013**, *46*, 1438.
- (2) (a) Drent, E.; van Dijk, R.; van Ginkel, R.; van Oort, B.; Pugh, R. I. *Chem. Commun.* **2002**, 744. (b) Drent, E.; van Dijk, R.; van Ginkel, R.; van Oort, B.; Pugh, R. I. *Chem. Commun.* **2002**, 964.
- (3) (a) Skupov, K. M.; Marella, P. R.; Simard, M.; Yap, G. P. A.; Allen, N.; Conner, D.; Goodall, B. L.; Claverie, J. P. *Macromol. Rapid Commun.* **2007**, *28*, 2033. (b) Skupov, K. M.; Piche, L.; Claverie, J. P. *Macromolecules* **2008**, *41*, 2309. (c) Piche, L.; Daigle, J.-C.; Poli, R.; Claverie, J. P. *Eur. J. Inorg. Chem.* **2010**, *2010*, 4595. (d) Daigle, J.-C.; Piche, L.; Claverie, J. P. *Macromolecules* **2011**, *44*, 1760. (e) Piche, L.; Daigle, J.-C.; Rehse, G.; Claverie, J. P. *Chem.—Eur. J.* **2012**, *18*, 3277. (f) Daigle, J.-C.; Piche, L.; Arnold, A.; Claverie, J. P. *ACS Macro Lett.* **2012**, *1*, 343.
- (4) (a) Luo, S.; Vela, J.; Lief, G. R.; Jordan, R. F. *J. Am. Chem. Soc.* **2007**, *129*, 8946. (b) Weng, W.; Shen, Z.; Jordan, R. F. *J. Am. Chem. Soc.* **2007**, *129*, 15450. (c) Vela, J.; Lief, G. R.; Shen, Z.; Jordan, R. F. *Organometallics* **2007**, *26*, 6624. (d) Shen, Z.; Jordan, R. F. *J. Am. Chem. Soc.* **2009**, *132*, 52. (e) Shen, Z.; Jordan, R. F. *Macromolecules* **2010**, *43*, 8706. (f) Conley, M. P.; Jordan, R. F. *Angew. Chem., Int. Ed.* **2011**, *50*, 3744. (g) Cai, Z.; Shen, Z.; Zhou, X.; Jordan, R. F. *ACS Catal.* **2012**, *2*, 1187.
- (5) (a) Guironnet, D.; Roesle, P.; Rünzi, T.; Göttker-Schnetmann, I.; Mecking, S. *J. Am. Chem. Soc.* **2009**, *131*, 422. (b) Rünzi, T.; Fröhlich, D.; Mecking, S. *J. Am. Chem. Soc.* **2010**, *132*, 17690. (c) Bouilhac, C. C.; Rünzi, T.; Mecking, S. *Macromolecules* **2010**, *43*, 3589. (d) Guironnet, D.; Caporaso, L.; Neuwald, B.; Göttker-Schnetmann,

I.; Cavallo, L.; Mecking, S. *J. Am. Chem. Soc.* **2010**, *132*, 4418. (e) Friedberger, T.; Wucher, P.; Mecking, S. *J. Am. Chem. Soc.* **2011**, *134*, 1010. (f) Leicht, H.; Göttker-Schnetmann, I.; Mecking, S. *Angew. Chem., Int. Ed.* **2013**, *52*, 3963.

(6) (a) Kochi, T.; Noda, S.; Yoshimura, K.; Nozaki, K. *J. Am. Chem. Soc.* **2007**, *129*, 8948. (b) Ito, S.; Munakata, K.; Nakamura, A.; Nozaki, K. *J. Am. Chem. Soc.* **2009**, *131*, 14606. (c) Noda, S.; Nakamura, A.; Kochi, T.; Chung, L. W.; Morokuma, K.; Nozaki, K. *J. Am. Chem. Soc.* **2009**, *131*, 14088. (d) Kanazawa, M.; Ito, S.; Nozaki, K. *Organometallics* **2011**, *30*, 6049.

(7) (a) Anselment, T. M. J.; Vagin, S. I.; Rieger, B. *Dalton Trans.* **2008**, 4537. (b) Anselment, T. M.; Anderson, C. E.; Rieger, B.; Boeddinghaus, M. B.; Fassler, T. F. *Dalton Trans.* **2011**, *40*, 8304. (c) Anselment, T. M. J.; Wichmann, C.; Anderson, C. E.; Herdtweck, E.; Rieger, B. *Organometallics* **2011**, *30*, 6602.

(8) (a) Borkar, S.; Newsham, D. K.; Sen, A. *Organometallics* **2008**, *27*, 3331. (b) Ravasio, A.; Boggioni, L.; Tritto, I. *Macromolecules* **2011**, *44*, 4180.

(9) (a) Hearley, A. K.; Nowack, R. J.; Rieger, B. *Organometallics* **2005**, *24*, 2755. (b) Haras, A.; Michalak, A.; Rieger, B.; Ziegler, T. *Organometallics* **2006**, *25*, 946. (c) Bettucci, L.; Bianchini, C.; Claver, C.; Suarez, E. J. G.; Ruiz, A.; Meli, A.; Oberhauser, W. *Dalton Trans.* **2007**, 5590. (d) Newsham, D. K.; Borkar, S.; Sen, A.; Conner, D. M.; Goodall, B. L. *Organometallics* **2007**, *26*, 3636. (e) Luo, R.; Newsham, D. K.; Sen, A. *Organometallics* **2009**, *28*, 6994. (f) Chen, C.; Anselment, T. M. J.; Fröhlich, R.; Rieger, B.; Kehr, G.; Erker, G. *Organometallics* **2011**, *30*, 5248.

(10) (a) Kochi, T.; Nakamura, A.; Ida, H.; Nozaki, K. *J. Am. Chem. Soc.* **2007**, *129*, 7770. (b) Nakamura, A.; Munakata, K.; Ito, S.; Kochi, T.; Chung, L. W.; Morokuma, K.; Nozaki, K. *J. Am. Chem. Soc.* **2011**, *133*, 6761. (c) Nakamura, A.; Kageyama, T.; Goto, H.; Carrow, B. P.; Ito, S.; Nozaki, K. *J. Am. Chem. Soc.* **2012**, *134*, 12366.

(11) Howell, J. A. S.; Palin, M. G.; Yates, P. C.; McArdle, P.; Cunningham, D.; Goldschmidt, Z.; Gottlieb, H. E.; Hezroni-Langerman, D. *J. Chem. Soc., Perkin Trans. 2* **1992**, 1769.

(12) These "(PO)PdMe" species are probably solvent adducts or, less likely, sulfonate-bridged dimers (see ref 4g).

(13) Neuwald, B.; Caporaso, L.; Cavallo, L.; Mecking, S. *J. Am. Chem. Soc.* **2013**, *135*, 1026.

(14) Haras, A.; Anderson, G. D. W.; Michalak, A.; Rieger, B.; Ziegler, T. *Organometallics* **2006**, *25*, 4491.

(15) (a) Espinet, P.; Albéniz, A. C.; Casares, J. A.; Martínez-Ilarduya, J. M. *Coord. Chem. Rev.* **2008**, *252*, 2180. (b) Hierso, J.-C. In *Science and Technology of Atomic, Molecular, Condensed Matter & Biological Systems*; Rubén, H. C., Ed.; Elsevier, 2013; Vol. 3, p 285. (c) Hierso, J.-C. *Chem. Rev.* **2014**, *114*, 4838.

(16) (a) Spannhoff, K.; Kuhl, N.; Kehr, G.; Fröhlich, R.; Erker, G. *J. Am. Chem. Soc.* **2009**, *131*, 17836. (b) Dodds, D. L.; Haddow, M. F.; Orpen, A. G.; Pringle, P. G.; Woodward, G. *Organometallics* **2006**, *25*, 5937.

(17) An O—O distance of 3.10 Å has been suggested as the cutoff for O—H...O hydrogen bonding. Khan, A. *J. Phys. Chem. B* **2000**, *104*, 11268.

(18) The (lone-pair)—P—C1 plane is defined as the plane that bisects the C15—P1—C8 angle. The other (lone-pair)—P—C_{ipso} planes are defined analogously.

(19) Howell, J. A. S.; Fey, N.; Lovatt, J. D.; Yates, P. C.; McArdle, P.; Cunningham, D.; Sadeh, E.; Gottlieb, H. E.; Goldschmidt, Z.; Hursthouse, M. B.; Light, M. E. *J. Chem. Soc., Dalton Trans.* **1999**, 3015.

(20) Bettucci, L.; Bianchini, C.; Meli, A.; Oberhauser, W. *J. Mol. Catal. A: Chem.* **2008**, *291*, 57.

(21) Bondi, A. *J. Phys. Chem.* **1964**, *68*, 441.

(22) (a) Hudnall, T. W.; Kim, Y.-M.; Bebbington, M. W. P.; Bourissou, D.; Gabbai, F. o. P. *J. Am. Chem. Soc.* **2008**, *130*, 10890. (b) Wade, C. R.; Zhao, H.; Gabbai, F. o. P. *Chem. Commun.* **2010**, 46, 6380. (c) Moebs-Sanchez, S.; Saffon, N.; Bouhadir, G.; Maron, L.; Bourissou, D. *Dalton Trans.* **2010**, 39, 4417. (d) Kim, Y.; Jordan, R. F. *Organometallics* **2011**, *30*, 4250.

- (23) Eapen, K. C.; Tamborski, C. J. *Fluorine Chem.* **1980**, *15*, 239.
- (24) (a) Mallory, F. B.; Mallory, C. W. Coupling Through Space in Organic Chemistry. In *Encyclopedia of Nuclear Magnet Resonance*; Grant, D. M.; Harris, R. K., Eds.; Wiley: Chichester, 1995; p 1491. (b) Kruck, M.; Munoz, M. P.; Bishop, H. L.; Frost, C. G.; Chapman, C. J.; Kociok-Köhn, G.; Butts, C. P.; Lloyd-Jones, G. C. *Chem.—Eur. J.* **2008**, *14*, 7808. (c) Bonnafoux, L.; Ernst, L.; Leroux, F. R.; Colobert, F. *Eur. J. Inorg. Chem.* **2011**, *2011*, 3387.
- (25) (a) Fey, N.; Howell, J. A.; Lovatt, J. D.; Yates, P. C.; Cunningham, D.; McArdle, P.; Gottlieb, H. E.; Coles, S. J. *Dalton Trans.* **2006**, 5464. (b) Mislow, K. *Acc. Chem. Res.* **1976**, *9*, 26.
- (26) Neuwald, B.; Falivene, L.; Caporaso, L.; Cavallo, L.; Mecking, S. *Chem.—Eur. J.* **2013**, *19*, 17773.
- (27) For an ideal boat conformation of the (PO-CF₃)Pd chelate ring in **3**, the Pd1, O1, C9, and C14 atoms would be coplanar and the corresponding dihedral angle Pd1–O1–C9–C14 would be 0°. In **3**, this dihedral angle is 7.3°. The corresponding dihedral angle in **4** is –4.8°.
- (28) (a) Sundquist, W. I.; Bancroft, D. P.; Lippard, S. J. *J. Am. Chem. Soc.* **1990**, *112*, 1590. (b) Mukhopadhyay, A.; Pal, S. *Eur. J. Inorg. Chem.* **2006**, *2006*, 4879. (c) Buckingham, A. D.; Stephens, P. J. *J. Chem. Soc.* **1964**, 4583. (d) Miller, R. G.; Stauffer, R. D.; Fahey, D. R.; Parnell, D. R. *J. Am. Chem. Soc.* **1970**, *92*, 1511. (e) Brookhart, M.; Green, M. L. H.; Parkin, G. *Proc. Natl. Acad. Sci. U.S.A.* **2007**, *104*, 6908. (f) Zhang, Y.; Lewis, J. C.; Bergman, R. G.; Ellman, J. A.; Oldfield, E. *Organometallics* **2006**, *25*, 3515.
- (29) Hierso, J.-C.; Fihri, A.; Ivanov, V. V.; Hanquet, B.; Pirio, N.; Donnadiou, B.; Rebière, B.; Amardeil, R.; Meunier, P. *J. Am. Chem. Soc.* **2004**, *126*, 11077.
- (30) Meier, U. W.; Hollmann, F.; Thewalt, U.; Klinga, M.; Leskelä, M.; Rieger, B. *Organometallics* **2003**, *22*, 3905.
- (31) Frew, J. J. R.; Damian, K.; Van Rensburg, H.; Slawin, A. M. Z.; Tooze, R. P.; Clarke, M. L. *Chem.—Eur. J.* **2009**, *15*, 10504.
- (32) (a) Perrin, C. L.; Dwyer, T. J. *Chem. Rev.* **1990**, *90*, 935. (b) Bodenhausen, G.; Ernst, R. R. *J. Am. Chem. Soc.* **1982**, *104*, 1304.
- (33) DFT analysis of the three coordinate species (2-{(o-CF₃-Ph)₂P}-benzenesulfonate)PdMe found that the *exo*₃ isomer is ca. 1.9 kcal/mol more stable than the *exo*₂ isomer. The *exo*₃ conformation was also found to be the most favorable for (2-{(o-CF₃-Ph)₂P}-benzenesulfonate)PdMe(ethylene). See ref 26.
- (34) Shanan-Atidi, H.; Bar-Eli, K. H. *J. Phys. Chem.* **1970**, *74*, 961.
- (35) As the temperature is decreased below –90 °C, the δ –53.2 resonance of *exo*₃-**4** broadens further, eventually broadening nearly fully into the baseline at –120 °C (Figure S14). This broadening is ascribed to restricted rotation of the CF₃ group. The ⁴J_{PF} coupling for the δ –53.2 resonance expected due to the *exo*-conformation of the corresponding CF₃ group is not observed, most likely due to the line broadening caused by restricted CF₃ rotation below ca. –90 °C and the *exo*₂-**4**/*exo*₃-**4** exchange above this temperature. The other ¹⁹F{¹H} resonances also broaden below –90 °C (the one at δ –56.9 most significantly) due to restricted CF₃ rotation.
- (36) The barrier for the exchange of the inequivalent CF₃ groups in the rapidly exchanging *exo*₂-**4**/*exo*₃-**4** mixture is in the range of that reported (ΔG[‡] > 18.2 kcal/mol) for CF₃ exchange of “(2-{(o-CF₃-Ph)₂P}-benzenesulfonate)PdMe”. This barrier was assigned to aryl rotation. See ref 12 and ref 13.
- (37) Siegel, J. S.; Anet, F. A. L. *J. Org. Chem.* **1988**, *53*, 2629.
- (38) Ladipo, F. T.; Anderson, G. K. *Organometallics* **1994**, *13*, 303.